Connected bulk negative index photonic metamaterials

Durdu Ö. Güney,[1,*] Thomas Koschny,[1,2] Maria Kafesaki,[2] and Costas M. Soukoulis[1,2]

[1]*Ames Laboratory, U.S. Department of Energy and Department of Physics and Astronomy, Iowa State University, Ames, Iowa 50011, USA*
[2]*Department of Materials Science and Technology, Institute of Electronic Structure and Laser, Foundation for Research and Technology Hellas (FORTH), University of Crete, 7110 Heraklion, Crete, Greece*
*Corresponding author: dguney@ameslab.gov

We show the designs of bulk one- and two-dimensionally isotropic photonic negative index metamaterials working around telecom wavelengths. The designed structures are inherently connected, which makes fabrication by direct laser writing and chemical vapor deposition or other techniques possible. © 2009 Optical Society of America

OCIS codes: 350.3618, 260.2065.

The simultaneously negative effective magnetic permeability and electric permittivity of metamaterials gives rise to exotic electromagnetic phenomena [1,2] not known to exist naturally. These materials enable a wide range of new applications as varied as cloaking devices and ultrahigh-resolution imaging systems. All photonic metamaterials at terahertz frequencies have been fabricated by well-established two-dimensional (2D) fabrication technologies, such as electron-beam lithography and evaporation of metal films, but they are one-dimensional (1D) designs with few functional layers [3,4]. A few efforts have been made to fabricate three to five layers [5,6], but this is also a 1D design. (We use the term "n-dimensional" ($n=1,2,3$) to describe a negative index metamaterial (NIM), operational for an n-dimensional space of k-vectors and use the term "bulk" for a metamaterial with multiple unit cells in all three directions.) However, bulk isotropic three-dimensional (3D) NIM designs with low absorption and high transmission that operate at terahertz and optical frequencies are needed to explore all potential applications of NIMs. Direct laser writing (DLW) is a more promising technique for the fabrication of truly 3D large-scale photonic metamaterials. Rill *et al.* [5] recently demonstrated the feasibility of this technique at near-IR frequencies assisted with silver chemical vapor deposition (CVD). In this Letter, we present the first truly bulk NIM design, which can potentially be fabricated with DLW around telecom wavelengths.

Designs of 3D isotropic NIMs exist, but fabricating them has remained a challenging task [6]. Only 2D isotropic NIMs are shown possible at microwave frequencies [7]. However, these designs cannot be miniaturized to give NIMs at terahertz and optical frequencies. Below, we describe new designs of both 1D and 2D isotropic negative index photonic metamaterials consisting of meandering wires. The inherent connectivity renders fabrication feasible by DLW and CVD. Lithography of bulk polymeric templates by DLW has widely been used [8] with sizes of less than 100 nm. By interconnecting the template, one can use CVD to cover it with a thin metallic film and obtain a bulk photonic metamaterial.

The design for 1D photonic NIM is illustrated in Fig. 1. It consists of a pair of gold meandering wires (radius 37 nm) embedded in a polyimide substrate, separated by a distance of 120 nm in the z direction. The Drude model is used to describe the metal. We assume experimental values for the plasma and the collision frequencies for bulk gold [3] ($\omega_p = 2\pi \times 2.175 \times 10^{15}$ s^{-1}, $\omega_c = 2\pi \times 6.5 \times 10^{12}$ s^{-1}). The dimensions of the unit cell are 220 nm $\times$ 240 nm $\times$ 320 nm. All of the bent cylindrical parts have the same curvature of 2/75 nm^{-1} at their center lines. The unit cell is designed to have inversion symmetry to allow for the homogeneous effective medium (HEM) approximation and retrieval of effective refractive index, electric permittivity, and magnetic permeability. See Fig. 1(b) for other parameters.

The incident field is configured as shown in Fig. 1(a). We use perfect electric conductor (PEC) and perfect magnetic conductor (PMC) boundary conditions. The magnetic resonance originates from the combined capacitance and inductance of the nanocircuit. The former results from the individual gaps and close proximity of the two meandering wires [see Fig. 1(b)], while the inner loops provide the latter. On the other hand, the nonresonant negative electric response arises from parallel currents oscillating along the continuous meandering wires.

All simulations were performed with the CST MICROWAVE STUDIO software package (Computer Simulation Technology GmbH, Darmstadt, Germany). The ratio of vacuum wavelength to unit cell size in the propagation direction is more than 6 at 215 THz (i.e., can be approximated by a HEM). The retrieved effective parameters [9] are shown as a function of frequency in Figs. 1(c)–1(e). Notice that both ϵ and μ are negative, and therefore n is also negative. The structure shown in ϵ and μ and the imaginary part of ϵ being negative is due to periodic effects [10]. The designed metamaterial structure has a negative index region with a bandwidth of 30 THz around 1.5 μm. The numerically calculated figure of merit (FOM)
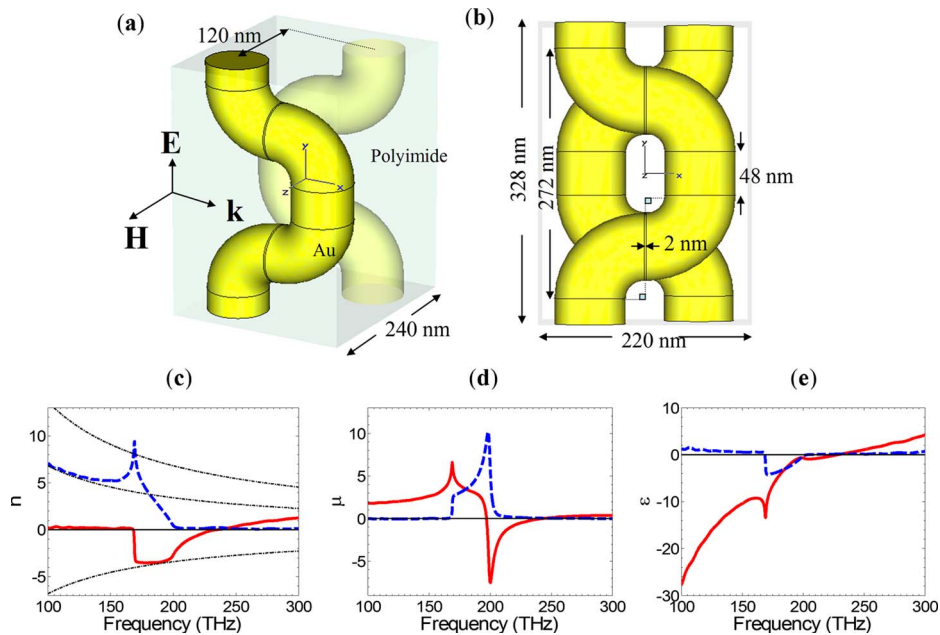
Fig. 1.   (Color online) (a), (b) Unit cell with parameters and incident field configuration for the 1D NIM consisting of one pair of meandering wires and (c)–(e) the corresponding retrieved effective parameters using the HEM approximation. The solid curves indicate the real parts, and the dashed curves indicate the imaginary parts.

[i.e., FOM defined as $-\mathrm{Re}(n)/\mathrm{Im}(n)$ at $\mathrm{Re}(n)=-1$] is 10 at 215 THz, where $n=-1$ (not optimized).

In the literature, it is the single-unit cell retrieval usually shown for metamaterials. However, this is not sufficient for a realistic large-scale metamaterial, because the corresponding multicell structure may not necessarily reproduce the electromagnetic properties expected from a single-unit cell.

In Fig. 2 we display the multiple unit cell results for the above 1D metamaterial and confirm the structure still preserves its negative index property in the region of interest (around 215 THz). In Fig. 2 the retrieved indices of refraction up to 11 unit cells are plotted in the same graph. Above 200 THz, the structure can be reasonably well approximated by an HEM. Thus, the results from the retrieval procedure for multiple unit cells closely follow the single-unit cell retrieval results and tend to coincide, except for an initial shift from single-unit cell to two unit cell curves. At the low frequency end of Fig. 2, where the index of refraction is positive, individual curves again tend to coincide (not shown). However, at intermediate frequencies, owing to the periodicity artifacts near the resonance, the effective medium approximation starts to break down and leads to relatively erratic behavior (therefore truncated).

Having discussed the 1D structure, we show that with using essentially the same meandering wires, it is possible to obtain a negative index of refraction in two propagation directions. For this purpose, we designed a 2D NIM unit cell with C4 symmetry as illustrated in Fig. 3. It consists of one pair of meandering wires with inversion symmetries in both x and z directions. The structure has a square lattice with a lattice constant $a=364$ nm. All other parameters are chosen to be the same as for the 1D case. The incident field is configured as shown in Fig. 3(a). We apply PEC and PMC boundary conditions to impose pe-

riodicity in nonincident directions. Although 2D periodic structures cannot necessarily be simulated by applying PEC/PMC boundary conditions, we found that the electromagnetic field cannot actually distinguish the symmetry in this specific structure.

The vacuum wavelength to unit cell size in propagation directions is about 5. The retrieved effective refractive index, magnetic permeability, and electric permittivity using the HEM approximation are displayed in Figs. 3(c)–3(e). Although the structure has room for further optimization, it already has an FOM of about 5, and the operation frequency lies close to the telecom band (150 THz) with about a 20 THz bandwidth. The designed structure has a 2D isotropy in the sense that it is symmetric under propagation in two directions with fixed polarization.

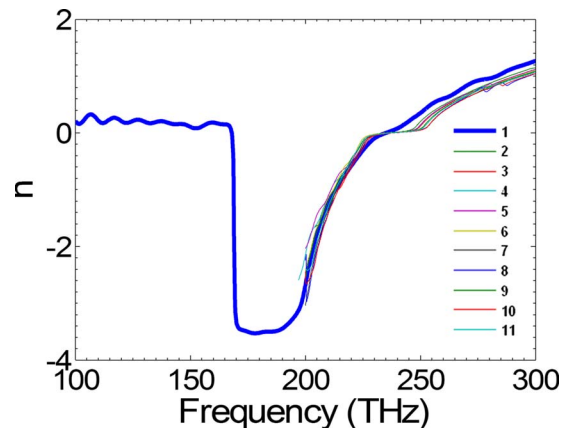In Fig. 4 we plot the multiple cell simulation results up to four unit cells. In contrast to the 1D struc-

Fig. 2.   (Color online) Retrieved effective index of refraction for different lengths (1 to 11 unit cells) plotted on the same graph. Curves for multiple unit cells (thin curves) tend to coincide, except for the initial shift from the single-unit cell curve (thick curve) to the two-unit cell curve.
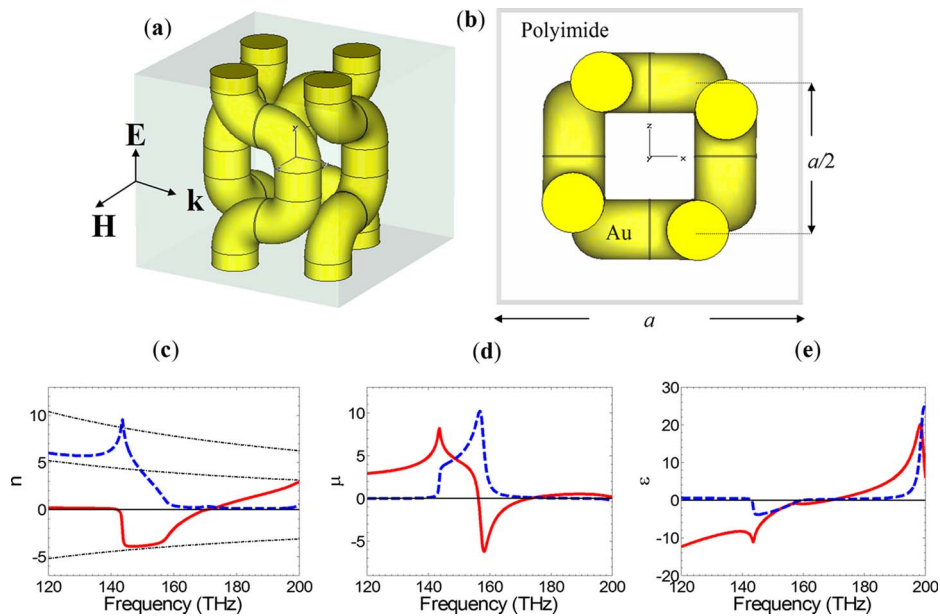
Fig. 3. (Color online) (a), (b) Unit cell and incident field configuration for the 2D NIM consisting of two pairs of meandering wires and (c)–(e) corresponding retrieved effective parameters using the HEM approximation.

ture, the 2D structure already homogenizes after a few number of unit cells. Like the 1D structure, however, the HEM approximation again starts to break down around the resonance below 160 THz and recovers at lower frequencies. Figure 4 shows the effective refractive index for different numbers of unit cells in the propagation direction, and one clearly sees how well the curves coincide.

In conclusion, we presented the designs of bulk 1D and 2D isotropic photonic metamaterials, which exhibit a negative index of refraction around the optical communication wavelength. Given state-of-the-art 2D fabrication technologies, manufacturability is still a concern to realize any practical optical devices based on metamaterials. Therefore, alternative technologies, such as DLW with compatible designs, are essential. Our design, owing to its inherently connected nature with the next-unit-cell neighbors, presents the first truly bulk photonic metamaterials feasible to fabricate with DLW and CVD. This may pave

the way to fabricate large-scale 3D metamaterials operating at optical frequencies and, therefore, all potential applications can become reality.
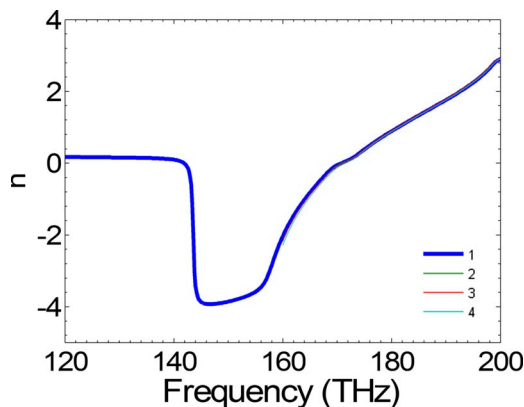
Fig. 4. (Color online) Retrieved effective index of refraction for the first four lengths (i.e., 1 to 4 unit cells) plotted on the same graph. Curves for multiple unit cells (thin curves) coincide with that of the single-unit cell (thick curve).

References

1. C. M. Soukoulis, S. Linden, and M. Wegener, Science **315**, 47 (2007).
2. V. M. Shalaev, Nat. Photonics **1**, 41 (2007).
3. G. Dolling, M. Wegener, and S. Linden, Opt. Lett. **32**, 551 (2007).
4. N. Liu, H. Guo, L. Fu, S. Kaiser, H. Schweizer, and H. Giessen, Nature Mater. **7**, 31 (2008).
5. M. S. Rill, C. Plet, M. Thiel, I. Staude, G. von Freymann, S. Linden, and M. Wegener, Nature Mater. **7**, 543 (2008).
6. Th. Koschny, L. Zhang, and C. M. Soukoulis, Phys. Rev. B **71**, 121103 (2005).
7. R. B. Greegor, C. G. Parazzoli, J. A. Nielsen, M. A. Thompson, M. H. Tanielian, and D. R. Smith, Appl. Phys. Lett. **87**, 091114 (2005).
8. M. Deubel, G. von Freymann, M. Wegener, S. Pereira, K. Busch, and C. M. Soukoulis, Nature Mater. **3**, 444 (2004).
9. D. R. Smith, S. Schultz, P. Markos, and C. M. Soukoulis, Phys. Rev. B **65**, 195104 (2001).
10. Th. Koschny, P. Markos, E. N. Economou, D. R. Smith, D. C. Vier, and C. M. Soukoulis, Phys. Rev. B **71**, 245105 (2005).